CHEMISTRY OF MATERIALS

VOLUME 19, NUMBER 16 AUGUST 7, 2007

Communications

Functional Template-Derived Poly(methyl methacrylate) Nanopillars for Solid-Phase Biological Reactions

Guofang Chen, Robin L. McCarley,* Steven A. Soper,* Catherine Situma, and Jowell G. Bolivar

Department of Chemistry and Center for Biomodular Multi-Scale Systems, Louisiana State University, Baton Rouge, Louisiana 70803

Received January 30, 2007
Revised Manuscript Received June 14, 2007

Here we demonstrate the unprecedented fabrication of free-standing, erect poly(methyl methacrylate), PMMA, nanopillar ensembles that possess ultrahigh aspect ratios (R = height/diameter; $5.7 \leq R \leq 343$) and the simple, nondestructive surface functionalization of the nanopillar ensembles. Photopolymerization of monomer within nanometer-diameter, micrometer-tall pores of anodic aluminum oxide (AAO) templates, followed by solution-phase release of the template and subsequent freeze-drying removal of solvent, leads to the facile production of PMMA nanostructures that retain the shape and size of the template pores. Use of traditional post-polymerization processing methods[1−4] results in collapse of the polymeric nanostructures. Both light-directed and solution-phase surface modification strategies[5] are found to be non-damaging to the PMMA nanopillars. The functionality of the high-surface-area PMMA is evidenced by outcomes from oligonucleotide hybridization events and proteolytic reactions on nanotextured modified surfaces. Finally, large area integration of the ultrahigh-aspect-ratio nanostructures (UHARNs) into PMMA-based microfluidic devices is easily achieved with simple, non-lithographic routes.[6]

The need for high-surface-area solid supports employed in bioreactor applications, which require minimal diffusional barriers or large target response signals, has led to investigations of a variety of materials as a support substrate for nucleic acids and immobilized enzymes/proteins.[7−10] Lithographically formed SiO_2 or Si nanopillars[11−13] are particularly attractive possibilities, because the load of biological reagent and diffusional attributes of the high-surface-area material would be defined by nanopillar geometry (pillar height, diameter, and spacing). However, the high cost and low throughput of nanolithography processes have led investigators to consider alternative routes.

* To whom correspondence should be addressed. E-mail: tunnel@lsu.edu; chsope@lsu.edu.

(1) Lee, W.; Jin, M.-K.; Yoo, W.-C.; Lee, J.-K. *Langmuir* **2004**, *20*, 7665−7669.
(2) Xiang, H.; Shin, K.; Kim, T.; Moon, S. I.; McCarthy, T. J.; Russell, T. P. *Macromolecules* **2004**, *37*, 5660−5664.
(3) Liang, Y.; Zhen, C.; Zou, D.; Xu, D. *J. Am. Chem. Soc.* **2004**, *126*, 16338−16339.
(4) Lee, W.; Scholz, R.; Goesele, K. *Angew. Chem., Int. Ed.* **2005**, *44*, 6050−6054.
(5) McCarley, R. L.; Vaidya, B.; Wei, S.; Smith, A. F.; Patel, A. B.; Feng, J.; Murphy, M. C.; Soper, S. A. *J. Am. Chem. Soc.* **2005**, *127*, 842−843.
(6) Hupert, M. L.; Guy, W. J.; Llopis, S. D.; Shadpour, H.; Rani, S.; Nikitopoulos, D. E.; Soper, S. A. *Microfluidics and Nanofluidics* **2006**, *3* (1), 1−11.
(7) Jeong, W. J.; Kim, J. Y.; Choo, J.; Lee, E. K.; Han, C. S.; Beebe, D. J.; Seong, G. H.; Lee, S. H. *Langmuir* **2005**, *21*, 3738−3741.
(8) Zhan, W.; Seong, G. H.; Crooks, R. M. *Anal. Chem.* **2002**, *74*, 4647−4652.
(9) Peterson, D. S.; Rohr, T.; Svec, F.; Fréchet, J. M. J. *Anal. Chem.* **2003**, *75*, 5328−5335.
(10) Kuwabara, K.; Ogino, M.; Motowaki, S.; Miyauchi, A. *Microelectron. Eng.* **2004**, *73−74*, 752−756.
(11) Kuo, C.-W.; Shiu, J.-Y.; Chen, P. *Chem. Mater.* **2003**, *15*, 2917−2920.
(12) Kaji, N.; Tezuka, Y.; Takamura, Y.; Ueda, M.; Nishimoto, T.; Nakanishi, H.; Horiike, Y.; Baba, Y. *Anal. Chem.* **2004**, *76*, 15−22.
(13) Craighead, H. G. *Science* **2000**, *290*, 1532−1535.

10.1021/cm0702870 CCC: $37.00
Published on Web 07/17/2007

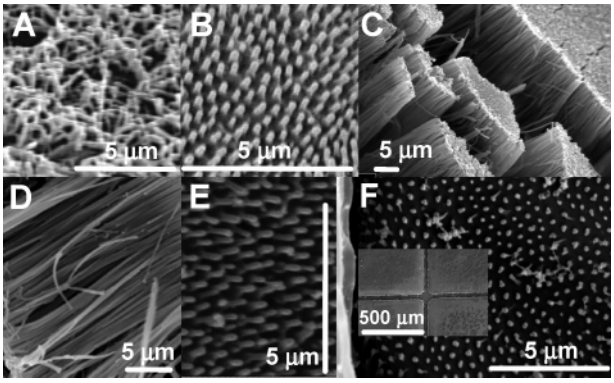

Figure 1. SEM images of PMMA nanopillars of varying aspect ratio, *R*. A. Top view of collapsed nanopillars (60-μm tall and 175-nm diameter, $R = 343$) resulting from NaOH template dissolution and subsequent ambient liquid removal. B. 1-μm tall and 175-nm diameter pillars, $R = 5.7$. C and D. $R = 343$. D. Close-up view of pillars in C. E. $R = 5.7$ pillars surface modified to yield carboxylic acid groups. F. Top view of 5-μm tall and 150-nm diameter ($R = 33.3$) nanopillars integrated into a 50-μm wide, 50-μm deep, and 5-cm long PMMA fluidic channel; the inset image is of the microchannel cross-tee containing free-standing nanopillars.

Template-based[14] embossing is a facile route for fashioning select polymers into pillar arrays[1,10,15] but has yet to provide supported, erect nanopillar arrays with high surface areas (ultrahigh aspect ratios) possessing the ability to withstand solution processing conditions required for their fabrication or immobilization of chemical and/or biological materials. The largest aspect ratio (282)[1] and, thus, surface area obtainable for polymeric nanopillars have to date been limited by the nature of the template fabrication method and the structural collapse of these features upon template removal.

We found that the use of rapid photopolymerization of methyl methacrylate in the pores of AAO[16,17] templates followed by template removal using the well-established sodium hydroxide (10 wt %) dissolution route[18] with subsequent ambient removal of solvent routinely resulted in complete collapse and disordering of the PMMA nanopillars, Figure 1A. Upon consideration of the possible causes of nanostructure collapse, surface tension effects were investigated. According to the lever principle,[19] the force F acting on the nanopillars during removal of the solvent is proportional to the cosine of the contact angle θ of the liquid with given surface tension γ and is also a function of the pillar aspect ratio R and the interpillar spacing d, as follows: $F = 2R\gamma(\cos\theta)/d$. To suppress this effect for pillars of a given R, γ must be reduced or the contact angle of the rinse liquid with respect to the nanostructures must be brought near 90° ($\cos\theta = 0$).

Through freeze-drying removal of the solvent at −80 °C and template etching with dilute H_3PO_4 (0.6 M) to minimize the force acting on the nanopillars (contact angle close to 90° under the above conditions),[19] it is possible to routinely form erect, ordered nanopillar ensembles with aspect ratios ranging from 5.7 (1-μm height, 175-nm diameter) to 343 (60-μm height, 175-nm diameter) as shown in Figure 1B−D; we have also constructed smaller diameter pillars, with dimensions down to 60 nm.[20] However, use of 10 wt % NaOH as the template etchant[18] leads to PMMA nanopillars that are severely deformed/collapsed; this can be attributed to the relatively hydrophilic surface of the PMMA nanopillars at high pH due to the presence of ionized, surface carboxylic acid groups[5] that are formed during the photopolymerization process.

Shown in Figure 1E is an electron micrograph of 1-μm-tall, 175-nm-diameter PMMA pillars that have been surface modified for 20 min using a direct-write UV photochemical patterning method that produces pendant, surface carboxylic acids, whose density is a function of the exposure time.[5] The ratio of oxygen to carbon on the surface of the PMMA nanopillars (as measured by X-ray photoelectron spectroscopy, XPS) increased when the UV modification time of the surface in air was increased from 0 to 20 min, which indicates introduction of oxygen into the polymer occurring during UV exposure, similar to what has been observed for planar PMMA in studies from our group.[5] This method results in nanometer-scale surface roughness increases for planar PMMA (associated with PMMA scission reactions[21]) that is exposure-time dependent. XPS data do not point to the presence of any remaining template material. Upon inspection of scanning electron microscopy (SEM) images for some of the smallest nanopillar feature sizes fabricated, little or no damage is apparent for exposure times up to 20 min (Figure 1E and Supporting Information), the time for production of maximum carboxylic acid surface density.[16] In addition, their surface exhibits higher water wettability (contact angle decreases from 99 ± 2° to 44 ± 2° following 20-min exposure), which is very beneficial for water-soluble molecule penetration into these three-dimensional networks. Furthermore, SEM images of nanopillars with activated surface carboxylic acid groups that have been reacted with amine-containing materials (proteins, oligonucleotides) and subsequently had the solvent removed using freeze drying prior to SEM imaging did not show signs of physical damage.

A characteristic limitation of microarray technologies is the upper limit of their dynamic range and sensitivity as a result of the maximum probe immobilization capacity of planar support surfaces. Our polymer nanopillar ensembles can increase these figures of merit via higher probe surface densities that result from the three-dimensional nature of each array element. For example, the surface areas of PMMA nanopillar ensembles with $R = 343$ and 5.7 are approximately 181 and 4 times that of planar PMMA.[22] The expected increase in "signal density" for oligonucleotide hybridization arrays that employ UHARN PMMA support

(14) Martin, C. R. *Science* **1994**, *266*, 1961−1966.
(15) Guo, C.; Feng, L.; Zhai, J.; Wang, G.; Song, Y.; Jiang, L.; Zhu, D. *ChemPhysChem* **2004**, *5*, 750−753.
(16) See Supporting Information.
(17) Masuda, H.; Fukuda, K. *Science* **1995**, *268*, 1466−1468.
(18) Lee, P.-S.; Lee, O.-J.; Hwang, S.-K.; Jung, S.-H.; Jee, S. E.; Lee, K.-H. *Chem. Mater.* **2005**, *17*, 6181−6185.
(19) Tanaka, T.; Morigami, M.; Atoda, N. *Jpn. J. Appl. Phys.* **1993**, *32*, 6059−6064.
(20) It was found that the height and the diameter of the nanopillars are uniform and dimensionally comparable to those of the original AAO template, pointing to little if any change in size of the polymeric nanostructures upon template removal.
(21) Wei, S.; Vaidya, B.; Patel, A. B.; Soper, S. A.; McCarley, R. L. *J. Phys. Chem. B* **2005**, *109*, 16988−16996.
(22) The surface roughness factor of sheet PMMA is typically found to be near 1.013. See Henry, A. C.; Tutt, T. J.; Galloway, M.; Davidson, Y. Y.; McWhorter, C. S.; Soper, S. A.; McCarley, R. L. *Anal. Chem.* **2000**, *72*, 5331−5337 for more details.

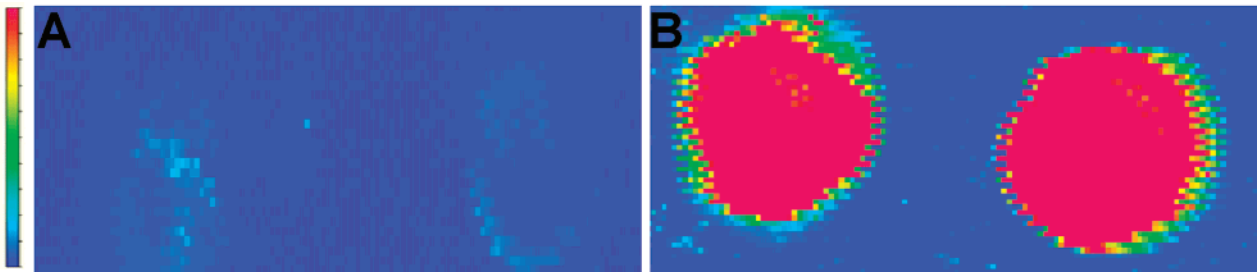

Figure 2. 13.2 mm × 3.06 mm fluorescence images of two-element oligonucleotide arrays on (A) planar PMMA and (B) nanopillared PMMA ($R = 343$) surfaces. Scale is 0 to 10 000 counts. Pixel size is 101.6 μm.

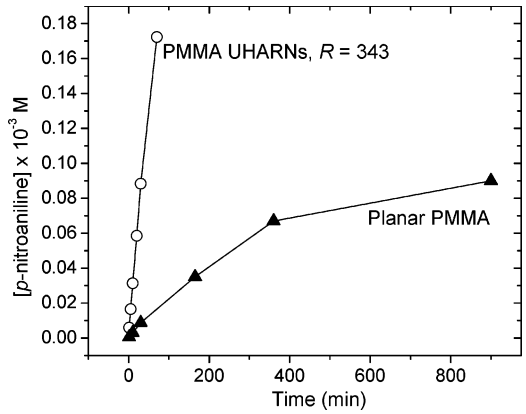

Figure 3. *p*-Nitroaniline formation from digestion of solution-phase *N*-α-benzoyl-L-arginine-*p*-nitroanilide (1×10^{-3} M) by covalently attached trypsin on PMMA substrates at 25 °C.

substrates is borne out upon examination of fluorescence microscopy images. In the case of the planar two-dimensional PMMA surface, the array generated weak fluorescence against a uniform background, Figure 2A. On the other hand, the fluorescence images resulting from the UHARN surface exhibited more intense fluorescence with well-defined and more uniform spots, with a normalized value of 3250 counts mm^{-2}. The signal enhancement was quantified,[16,23] and the average volumetric fluorescence value for the nanostructured PMMA substrate (2.36×10^7) is 110 times that for planar PMMA (2.15×10^5), a highly significant improvement.

The amount of substrate processed in a given time by enzymes immobilized to a surface with a fixed two-dimensional footprint can be substantially increased through the use of nanopillar supports, as evidenced in Figure 3. From substrate concentration studies, the magnitude of the kinetic parameter, V_{max}, for digestion of *N*-α-benzoyl-L-arginine-*p*-nitroanilide to yield *p*-nitroaniline was found to be ~10 times greater for trypsin covalently attached to PMMA UHARN (51.8 μM min^{-1}, $R = 343$) versus planar PMMA (5.02 μM min^{-1}) supports. This ability to process a large amount of solution-phase substrate in a given two-dimensional domain bodes well for flow-through bio-reactors in microfluidic devices where high sample processing speeds are important and will be further augmented by the decreased diffusional distances required for targets locating their enzyme reaction partners, thereby minimizing diffusion-defined kinetic constraints.[24]

A key issue in the fabrication of microfluidic devices is the straightforward incorporation of elements that result in device functionality for the end user. To that end, by using the simple method of micromilling[6] applied to the AAO template prior to methyl methacrylate polymerization, we have been able to readily integrate free-standing polymer nanopillars directly into PMMA microfluidic channels, as shown in Figure 1F.

The approach described here for the fabrication of structurally robust and functional high-surface-area polymeric nanostructures paves the path toward development of modular microfluidics-based processing assays, which require highly accessible surface-immobilized reactants in a small footprint, such as microarrays and solid-phase enzymatic reactors. In preliminary experiments, we have found that functional microfluidic devices made with this method can be used to sort DNA. In addition, we are exploiting the generality of the approach by using modified poly(carbonate) and cyclic olefin copolymer UHARN devices for the capture of low-abundance proteins and nucleic acids.

Acknowledgment. We thank S. B. Lee and S. J. Son at the University of Maryland for discussions regarding the fabrication of anodic alumina and J. Chao at LSU for assistance with the SEM measurements. This work was supported by NIH and NSF.

Supporting Information Available: Experimental details (PDF). This material is available free of charge via the Internet at http://pubs.acs.org.

CM0702870

(23) Chen, W.; Westerhoff, P.; Leenheer, J. A.; Booksh, K. *Environ. Sci. Technol.* **2003**, *37*, 5701−5710.

(24) The general utility of the UHARN bioreactor was further demonstrated by digestion of myoglobin and cytochrome C. See Supporting Information for more details.